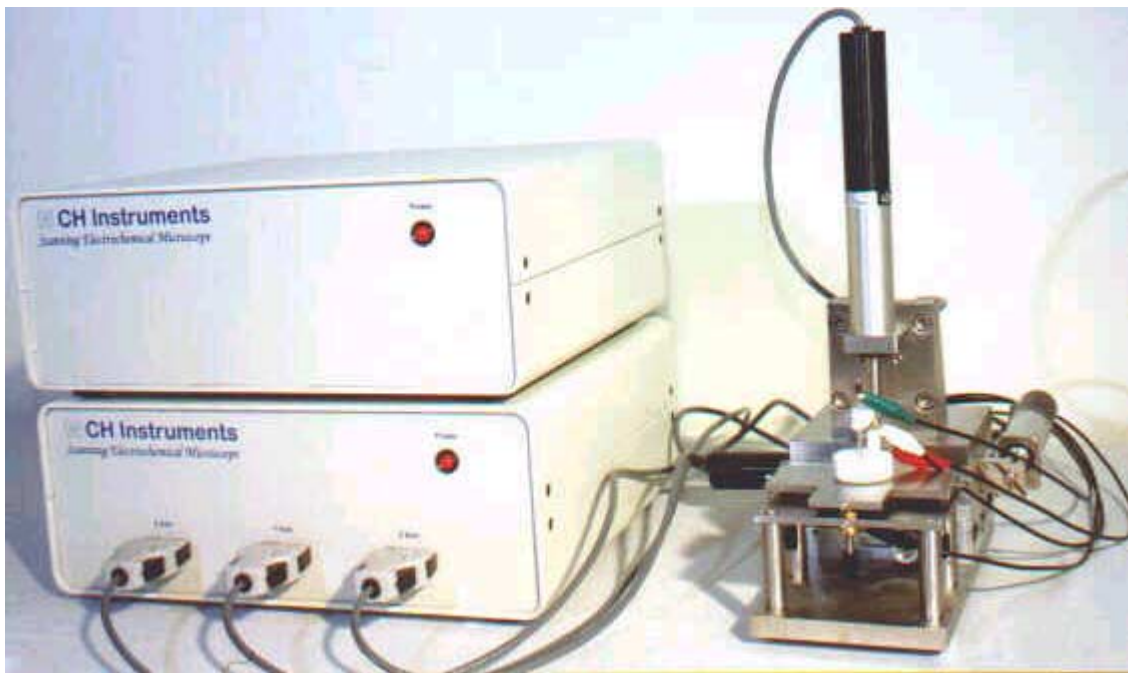


# Scanning Electrochemical Microscope



**CH Instruments**

# Overview

The scanning electrochemical microscope (SECM) was introduced in 1989<sup>1</sup> as an instrument that could examine chemistry at high resolution near interfaces. It is based on reactions that occur at a small electrode (the tip) as it is scanned in close proximity to a surface. SECM can be employed to obtain chemical reactivity images of surfaces and also in quantitative measurements of reaction rates. Numerous studies with the SECM have now been reported from a number of laboratories all over the world and the instrument has been used for a wide range of applications, including studies of corrosion, biological systems (e.g., enzymes, skin, leaves), membranes and liquid/liquid interfaces<sup>2</sup>. Trapping and electrochemical detection of single molecules with the SECM has also been reported. With the introduction of the CHI900 SECM, developed in collaboration with the University of Texas group, this technique now becomes available to any laboratory.

The CHI900 Scanning Electrochemical Microscope consists of a digital function generator, a bipotentiostat, high resolution data acquisition circuitry, a three dimensional micropositioner, an Inchworm motor controller, and sample and cell holder. The diagrams of SECM and cell/sample holder are shown below. The three dimensional micropositioner has a spatial resolution better than one nanometer but it allows a maximum traveling distance of several centimeters. The potential control range of the bipotentiostat is  $\pm 3.275\text{V}$  and the current range is  $\pm 10\text{mA}$ . The instrument is capable of measuring current down to sub-picoamperes.

In addition to SECM imaging, two other modes of operation are provided for scanning probe applications: the Probe Scan Curve mode and the Probe Approach Curve mode. The Probe Scan Curve mode allows the probe to move in X, Y, or Z direction while the probe and substrate potentials are controlled and currents are measured. The probe can be stopped when current reaches a specified level. This is particularly useful in searching for an object on the surface and determining approach curves. The Probe Approach Curve mode allows the probe to approach the surface of the substrate. It is also very useful in distinguishing the surface process. The PID control is used in this case. It automatically adjusts the step size to allow fast surface approach yet without the probe touching the surface.

The CHI900 is designed for scanning electrochemical microscopy, but many conventional electrochemical techniques are also integrated for convenience, such as CV, LSV, CA, CC, DPV, NPV, i-t, DPA, and TPA. The bipotentiostat works for CV, LSV, DPV, and for amperometric i-t curves. In CV, LSV and DPV, the potential of both channels can be scanned simultaneously.

The instrument is controlled by an external PC under a Windows environment. It is easy to install and use. No plug-in card or other hardware is required on the PC side. The user interface follows the Windows application design guide. If you are familiar with Windows application, you can use the software even without an operation manual or on-line help. The commands, parameters, and options use terminology that is familiar to most chemists. The toolbar allows quick access to the most commonly used commands. The help system provides context sensitive help. It is systematic and complete.

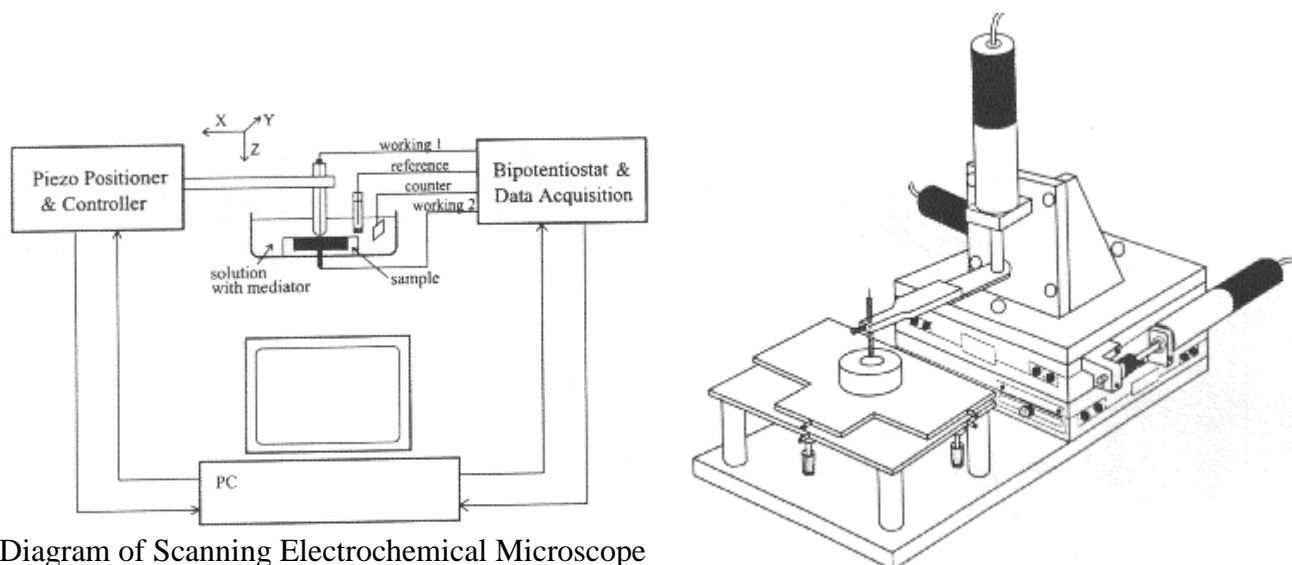


Diagram of Scanning Electrochemical Microscope Cell/Sample Holder

The instrument provides many powerful functions, such as file handling, experimental control, graphics, data analyses, and digital simulation. Some of the unique features include macro command, working electrode conditioning, color, legend and font selection, data interpolation, visual baseline correction, signal averaging, Fourier spectrum, and equations relating to electrochemical techniques.

1. A. J. Bard, F.-R. F. Fan, J. Kwak, and O. Lev, *Anal. Chem.* **61**, 132 (1989); U.S. Patent No. 5,202,004 (April 13, 1993).
2. A. J. Bard, F.-R. Fan, M. V. Mirkin, in *Electroanalytical Chemistry*, A. J. Bard, Ed., Marcel Dekker, New York, 1994, Vol. 18, pp 243-373.

## CHI900 SECM Specifications

### Micropositioner:

- X, Y, Z Resolution: < 1 nm
- X, Y, Z Total Travel: 2.5 cm (5.0 cm optional)

### Bipotentiostat:

- Probe Potential:  $\pm 3.275$  V
- Substrate Potential:  $\pm 3.275$  V
- Compliance Voltage:  $\pm 12$  V
- Current Sensitivity:  $10^{-12}$  A/V to  $10^{-3}$  A/V
- Maximum Current:  $\pm 10$  mA
- Low Current Measurability: < 1 pA
- ADC Resolution: 20-bit @ 1kHz, 24-bit @ 10 Hz

### Other Features:

- Real Time Absolute and Relative Distance Display
- Real Time Probe and Substrate Current Display

## Applications

- Electrode surface studies
- Corrosion
- Biological samples
- Solid dissolution
- Liquid/liquid interfaces
- Membranes

## Techniques

### Scanning Probe Techniques

- Probe Scan Curve (X, Y and Z directions)
- Probe Approach Curve
- Scanning Electrochemical Microscope

### Sweep Techniques

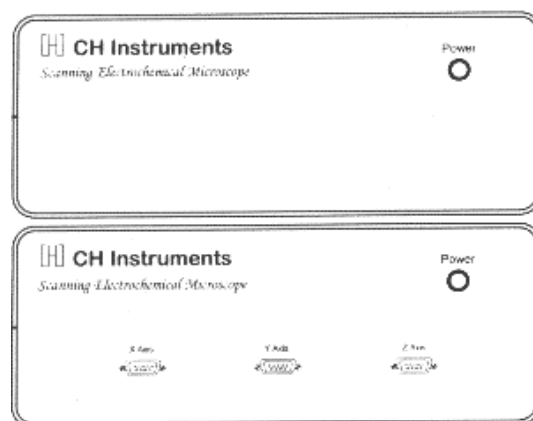
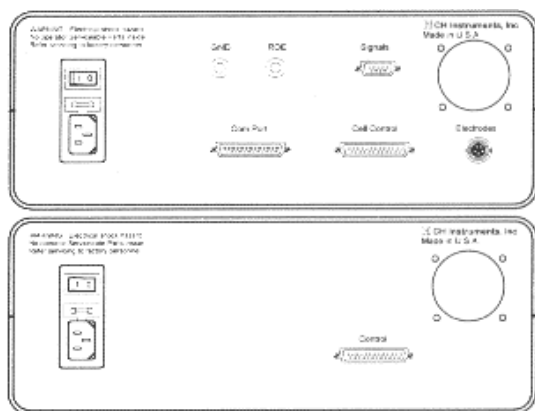
- Cyclic Voltammetry
- Linear Sweep Voltammetry

### Step and Pulse Techniques

- Chronoamperometry
- Chronocoulometry
- Differential Pulse Voltammetry
- Normal Pulse Voltammetry
- Square Wave Voltammetry

### Other Techniques

- Amperometric i-t Curve
- Differential Pulse Amperometry
- Double Differential Pulse Amperometry
- Triple Pulse Amperometry
- Bulk Electrolysis with Coulometry
- Various Stripping Voltammetry
- Potentiometry



Bipotentiostat (Top) and Motor Controller (Bottom)

# Highlights

## User Interface

- **32-bit Windows application**
- **Multi-Document Interface**
- **toolbar:** quick access to frequently used commands
- **status bar:** technique and command prompt
- **pull-down menus**
- **WYSIWYG graphics**
- **comprehensive and context sensitive help**

## File Management

- **reopen saved data files**
- **save data file**
- **delete files**
- **list data file**
- **convert to text files:** for exporting data to other software, such as spreadsheets
- **text file format**
- **print present data**
- **print multiple data files**
- **print setup**

## Setup

- **technique:** scanning probe and many other EC techniques
- **experimental parameters:** extremely wide dynamic range
- **system setup:** choice of communication port, choice polarity of potential and current axis

- **hardware test:** digital and analog circuitry diagnostic test

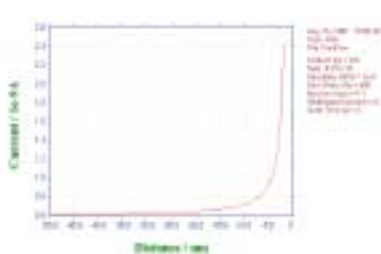
## Instrument Control

- **run experiment:** real time data display in most cases
- **pause/resume during run**
- **stop running experiment**
- **reverse scan direction during run:** for cyclic voltammetry
- **repetitive runs:** automatic data save, signal averaging, delay or prompt between runs, up to 999 runs
- **run status:** stir, purge, smooth after run, SMDE control status
- **macro commands:** edit, save, read, and execute a series of commands
- **open circuit potential measurement**
- **analog filter setting:** automatic or manual setting of signal filters for both current channels
- **cell control:** purge, stir, cell on, SMDE drop collection, and pre-run drop knock.
- **step functions:** initial and two step potentials, duration of steps and number of steps, particularly useful for electrode treatment
- **working electrode conditioning before running experiment:** programmable 3 steps

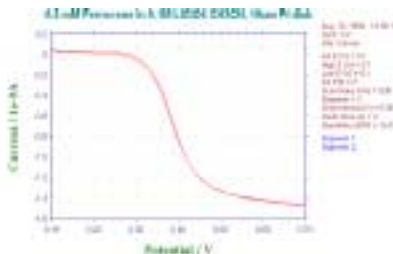
- **stripping mode:** enable/disable, deposition potential and time, stir and purge conditions
- **SECM probe:** motor calibration, probe travel, probe absolute and relative position, position re-zero, forward and reverse distance ratio

## Graphic Display

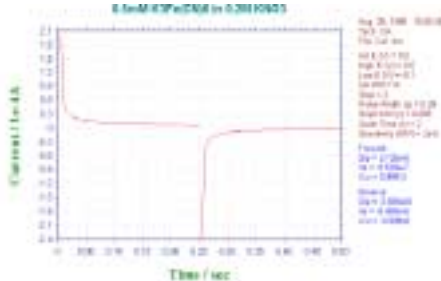
- **present data plot**
- **3D surface plot:** front, rear, side, top and bottom view
- **overlay plots:** several sets of data overlaid for comparison
- **add data to overlay:** adding data files to overlay plot, files from different directories can be selected
- **parallel plots:** several sets of data plotted side by side
- **add data to parallel:** adding data files to parallel plot, files from different directories can be selected, position of each plot can be controlled
- **zoom in/out:** visually selected zoom area
- **manual results:** visually selected baseline
- **peak definition:** shape, width, and report options
- **Special Plots:** x-y,  $i_p$ -v,  $i_p$ -v<sup>1/2</sup>,  $E_p$ -log v, and semilog plots



PAC at a conductive substrate.



CV at a 10µm Pt tip.



Chronoamperometry data.

# Highlights

- **graph options:** video or printer options, axis, parameters, baseline, results, grids, axis inversion, axis freeze, axis titles, data sets, XY scales, current density option, reference electrode, header, and notes
- **color and legend:** background, axis, grid, curves, legend size, thickness, color or monochrome scale bar and display intervals
- **font:** font, style, size and color for axis labels, axis titles, header, parameters, and results
- **copy to clipboard:** for pasting the data plot to word processors

## Data Processing

- **smoothing:** 5-49 point least square and Fourier transform
- **derivatives:** 1st - 5th order, 5-49 point least square
- **integration**
- **convolution:** semi-derivative and semi-integral
- **interpolation:** 2 $\times$  - 64 $\times$  data interpolation
- **baseline correction:** visually selected baseline, slope and dc level compensation
- **data point removing**
- **data point modifying:** visual data point modification
- **background subtraction:** difference of two sets of data
- **signal averaging**

- **mathematical operations:** both X and Y data array
- **Fourier spectrum**

## Digital Simulation

- **fast implicit finite difference algorithm**
- **reaction mechanisms:** 10 predefined mechanisms; any combination involving electron transfer, first- and second-order chemical reactions
- **system:** diffusive or adsorptive
- **maximum equations:** 12
- **maximum species:** 9
- **simulation parameters:** standard redox potentials, rate of electron transfer, transfer coefficient, concentration, diffusion coefficient, forward and reverse chemical reaction rate constants, temperature, electrode area, and experimental parameters
- **save simulation parameters**
- **read simulation parameters**
- **real time data display**
- **real time display of concentration profiles**
- **automatic search and determine over-determined equilibrium constants**
- **dimensionless current**

- **equilibrium data**

## View

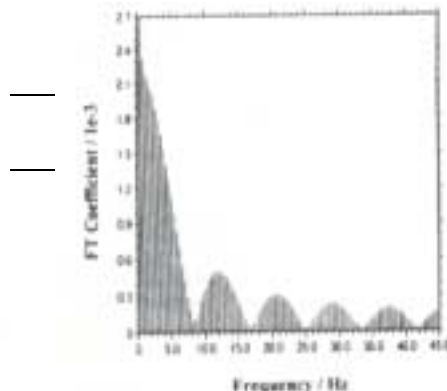
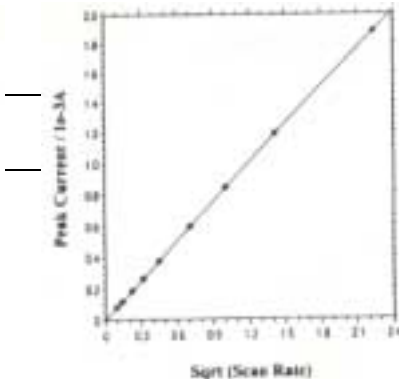
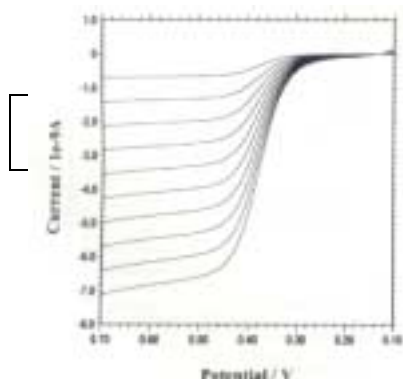
- **data information:** date, time, filename, data source, instrument model, data processing performed, header and notes
- **data listing:** data information and numerical data array
- **equations:** general equations and equations relating to various electrochemical techniques
- **clock**
- **SECM probe status:** probe position and current display
- **toolbar**
- **status bar**

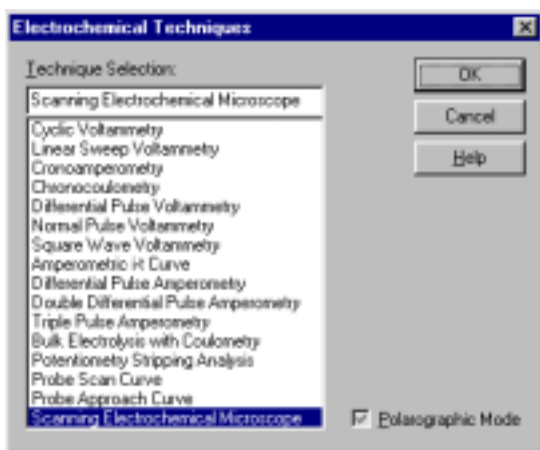
## Help

- **context sensitive help**
- **help topics**
- **about the application**

## System requirements

- **operating system:** Microsoft Windows 95
- **processor:** Pentium
- **RAM:** 16 M bytes
- **monitor:** VGA
- **mouse**
- **serial communication port**
- **output device:** any printer or plotter supported by Windows





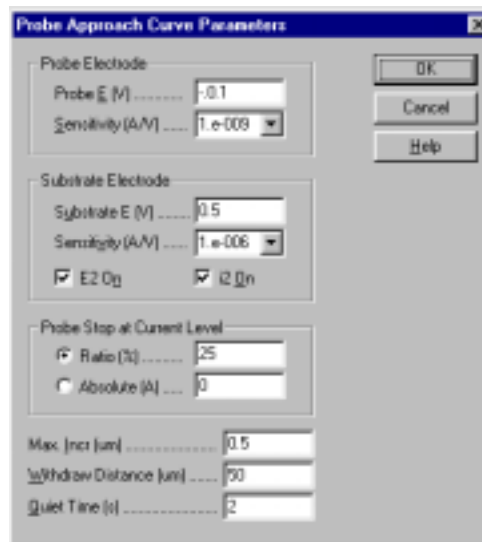
A large repertoire of electrochemical techniques.



System setup allows any convention of current and potential polarity.



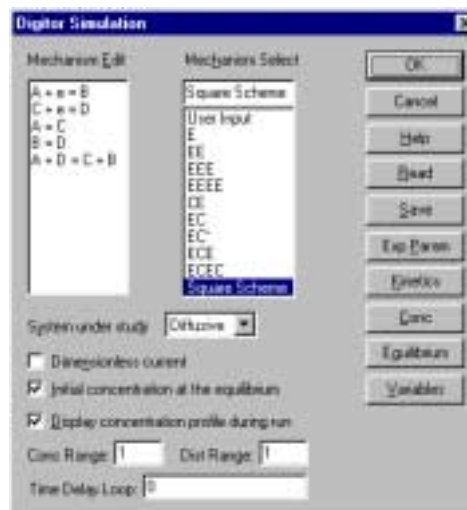
Experimental parameter dialog box for Probe Scan Curve.



Experimental parameter dialog box for Probe Approach Curve.

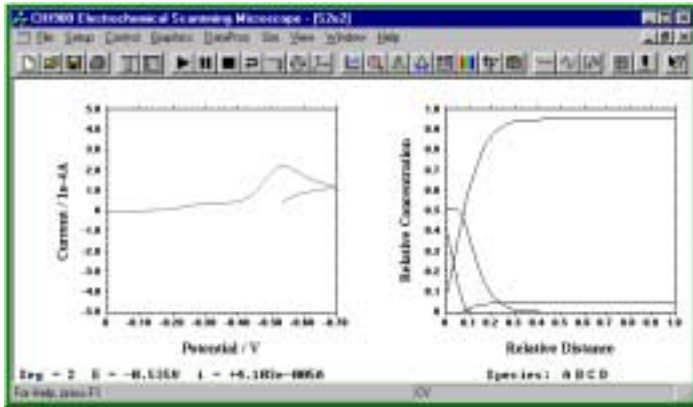


Experimental parameter dialog box for SECM.



User interface for digital simulator.

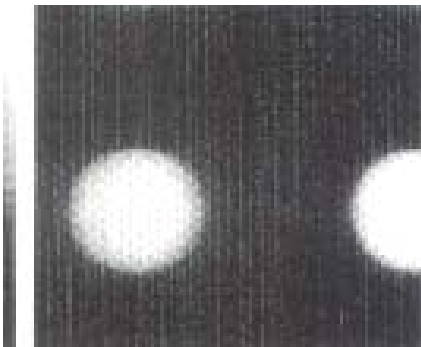
# Highlights



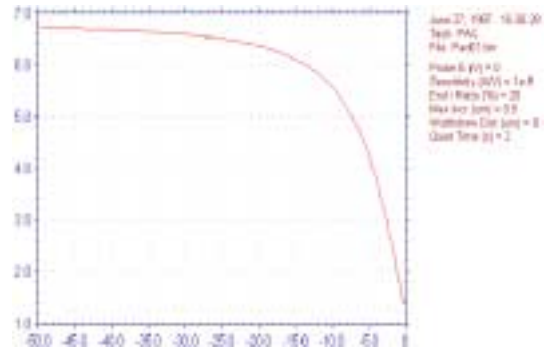
Digital Simulator displays both current response and the concentration profiles of different species during the simulation process.



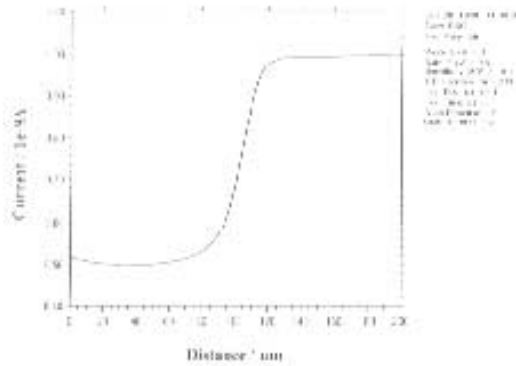
Equations relating to various techniques can be viewed on line.



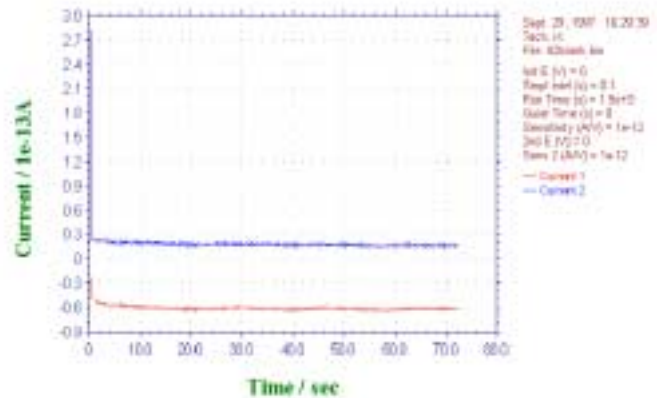
SECM image of microelectrode array.



Probe Approach Curve at insulating substrate.



Probe Scan Curve across insulator/conductor boundary.



Instrument noise level of both channels.

# Principle and Applications of SECM

## I. Operational Principles of SECM

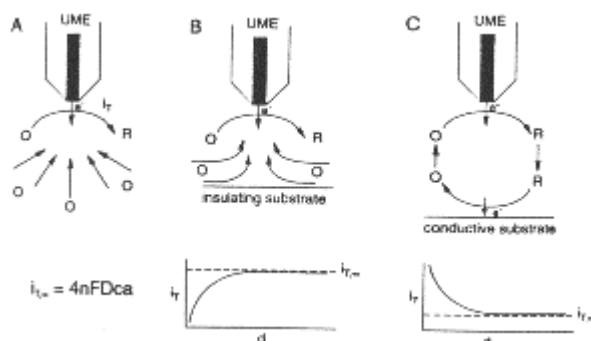
As in other types of scanning probe microscopes, SECM is based on the movement of a very small electrode (the tip) near the surface of a conductive or insulating substrate.<sup>1</sup> In amperometric SECM experiments, the tip is usually a conventional ultramicroelectrode (UME) fabricated as a conductive disk of metal or carbon in an insulating sheath of glass or polymer. Potentiometric SECM experiments with ion-selective tips are also possible.<sup>2</sup>

In amperometric experiments, the tip current is perturbed by the presence of the substrate. When the tip is far (i.e. greater than several tip diameters) from the substrate, as shown in Fig. 1A, the steady-state current,  $i_{T,\infty}$ , is given by

$$i_{T,\infty} = 4nFDc_a$$

in which  $F$  is the Faraday constant,  $n$  the number of electrons transferred in the tip reaction ( $O + ne \rightarrow R$ ),  $D$  the diffusion coefficient of species  $O$ ,  $C$  is the concentration, and  $a$  is the tip radius. When the tip is moved toward the surface of an insulating substrate, the tip current,  $i_T$ , decreases because the insulating sheath of the tip blocks diffusion of  $O$  to the tip from the bulk solution. The closer the tip gets to the substrate, the smaller  $i_T$  becomes (Fig 1B). On the other hand, with a conductive substrate, species  $R$  can be oxidized back to  $O$ . This produces an additional flux of  $O$  to the tip and hence an increase in  $i_T$  (Fig. 1C). In this case, the smaller is the value of  $d$ , the larger is  $i_T$ , with  $i_T \rightarrow \infty$  as  $d \rightarrow 0$ , if the oxidation of  $R$  on the substrate is diffusion-limited. These simple principles form the basis for the feedback mode of the SECM operations.

**Figure 1.** Operating with UME far from the substrate leads to a steady-state current near an insulating substrate, leads to  $i_T < i_{T,\infty}$ ; (C) with substrate, positive feedback



principles of SECM: (A). substrate, diffusion of  $O$  current,  $i_{T,\infty}$ ; (B). with UME hindered diffusion of  $O$  UME near a conductive of  $O$  leads to  $i_T > i_{T,\infty}$ .

When the tip is rastered in the x-y plane above the substrate, the tip current variation represents changes in topography or conductivity (or reactivity). One can separate topographic effects from conductivity effects by noting that over an insulator  $i_T$  is always less than  $i_{T,\infty}$ , while over a conductor  $i_T$  is always greater than  $i_{T,\infty}$ .

In the feedback mode of the SECM operation as stated above, the overall redox process is essentially confined to the thin layer between the tip and the substrate. In the substrate-generation/tip-collection (SG/TC) mode (when the substrate is a generator and the tip is a collector), the tip travels within a thin diffusion layer generated by the substrate electrode.<sup>1b,3</sup> There are some shortcomings which limit the applicability of the SG/TC mode if the substrate is large: (1). the process at a large substrate is always non-steady state; (2). a large substrate current may cause significant  $iR$ -drop; and (3). the collection efficiency, i.e., the ratio of the tip current to the substrate current, is low. The tip-generation/substrate-collection (TG/SC) mode is advisable for kinetic measurements, while SG/TC can be used for monitoring enzymatic reactions, corrosion, and other heterogeneous processes at the substrate surface.

## II. Applications

### A. Imaging and positioning

A three-dimensional SECM image is obtained by scanning the tip in the x-y plane and monitoring the tip





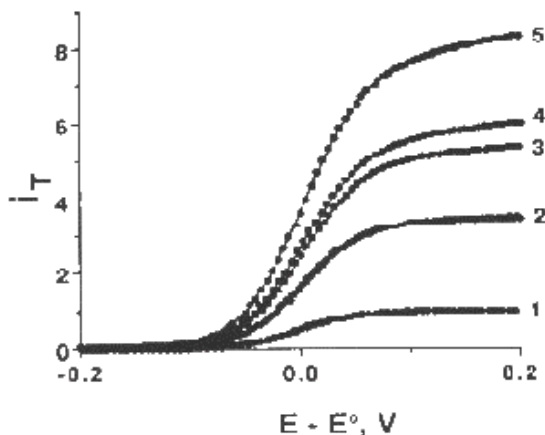
**Figure 2.** SECM image of a polycarbonate filtration membrane with a 2- $\mu\text{m}$ -diameter Pt disk UME in  $\text{Fe}(\text{CN})_6^{4-}$  solution. Average pore diameter is ca. 10  $\mu\text{m}$ .

The oxidation of ferrocene at a Pt UME has been carried out.<sup>4c</sup> Five steady-state voltammograms obtained at different distances are shown in Fig. 3, along with the theoretical curves calculated with the values of the kinetic parameters extracted from the quartile potentials. The heterogeneous rate constant, current,  $i_T$ , as a function of tip location. A particular advantage of SECM in imaging applications, compared to other types of scanning probe microscopy, is that the response observed can be interpreted based on fairly rigorous theory, and hence the measured current can be employed to estimate the tip-substrate distance. Moreover, SECM can be used to image the surfaces of different types of substrates, both conductors and insulators, immersed in solutions. The resolution attainable with SECM depends upon the tip radius. For example, Fig. 2 shows one SECM image of a filtration membrane obtained with a 2- $\mu\text{m}$ -diameter Pt disk tip in  $\text{Fe}(\text{CN})_6^{4-}$  solution. Average pore diameter is ca. 10  $\mu\text{m}$ . An image demonstrating the local activity of an enzymatic reaction on a filtration membrane is shown in Fig. 9 as described below.

### B. Studies of heterogeneous electron transfer reactions

SECM has been employed in heterogeneous kinetic studies on various metal, carbon and semiconductor substrates.<sup>4</sup> In this application, the x-y scanning feature of SECM is usually not used. In this mode, SECM has many features of UME and thin layer electrochemistry with a number of advantages. For example, the characteristic flux to an UME spaced a distance,  $d$ , from a conductive substrate is of the order of  $DC/d$ , independent of the tip radius,  $a$ , when  $d < a$ . Thus, very high fluxes and thus high currents can be obtained. For example, the measurement of the very fast kinetics of  $k^0$ , obtained ( $3.7 \pm 0.6 \text{ cm/sec}$ ) remains constant within the range of experimental error, while the mass-transfer rate increases with a decrease in  $d$ .

**Figure 3.** Tip steady-state oxidation of 5.8 mM ferrocene at a 1.1- $\mu\text{m}$ -radius Pt tip. Solid and solid circles are substrate separation decreases 0.17, 0.14, and 0.1). (Reprinted copyright 1993, American



voltammograms for the in 0.52 M TBABF<sub>4</sub> in MeCN lines are theoretical curves experimental data. Tip- from 1 to 5 ( $d/a = \infty, 0.27$ , with permission from Ref. 4e, Chemical Society.)

### C. Studies of homogeneous

As mentioned above, the (substrate) mode of SECM, in rotating ring disk electrode suitable for the studies of kinetics.<sup>1b,5</sup> The SECM approach has the advantage that different substrates can be examined easily, i.e., without the need to construct rather difficult to fabricate RRDEs, and higher interelectrode fluxes are available without the need to rotate the electrode or otherwise cause convection in the solution. Moreover, in the TG/SC mode, the collection efficiency in the absence of perturbing homogeneous chemical reaction is near 100%, compared to significantly lower values in practical RRDEs. Finally, although transient SECM measurements are possible, most applications have involved steady-state currents, which are easier to measure and are not perturbed by factors like double-layer charging and also allow for signal averaging. For example, the reductive coupling of both dimethylfumarate (DF) and fumaronitrile (FN) in N,N-dimethyl formamide has been studied with the TG/SC mode.<sup>5a</sup> Fig. 4 shows tip and substrate steady-state voltammograms for the TG/SC regime. Comparable values of both of the plateau currents indicated that the mass transfer rate was sufficiently fast to study the rapid homogeneous reaction. From the approach curves of both tip and substrate currents (Fig. 5) obtained at various FN concentrations, a rate constant  $k_c = 2.0 (\pm 0.4) \times 10^5 \text{ M}^{-1}\text{s}^{-1}$  was determined for the dimerization reactions.

### chemical reactions

TG/SC (with small tip and the same manner as the (RRDE), is particularly homogeneous chemical

**Figure 4.** SECM (28.2 mM) reduction in  $E_T$  was scanned at 100 AgQRE. (Reprinted with copyright 1992, American

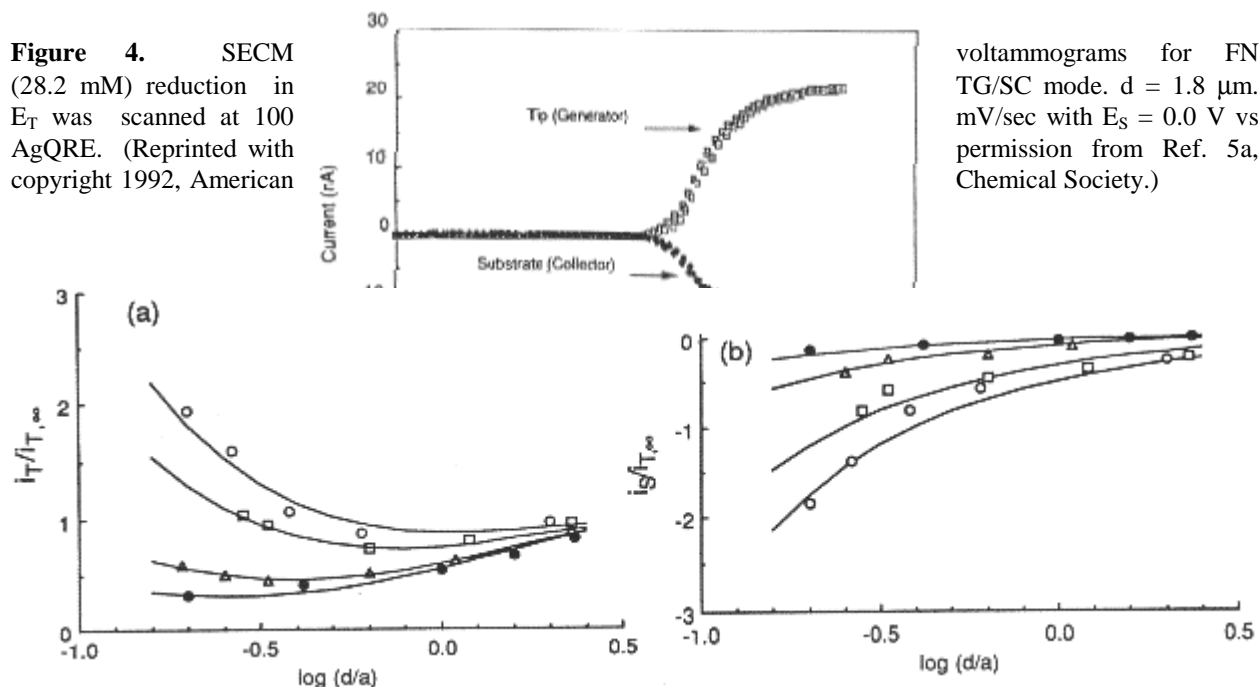


**Figure 5.** Normalized tip (generation, A) and substrate (collection, B) current-distance behavior for FN reduction. FN concentration: (open circle) 1.50 mM, (open square) 4.12 mM, (open triangle) 28.2 mM, and (filled circle) 121 mM.  $a = 5 \mu\text{m}$ , substrate radius is  $50 \mu\text{m}$ . The solid lines represent the best theoretical fit for each set of data. (Reprinted with permission from Ref. 5a, copyright 1992, American Chemical Society.)

#### D. Characterization of thin films and membranes

SECM is also a useful technique for studying thin films on interfaces. Both mediated and direct electrochemical measurements in thin films or membranes can be carried out. For example, polyelectrolytes, electronically conductive polymers, passivation films on metals and dissolution processes have been investigated by SECM.<sup>6</sup> A unique type of cyclic voltammetry, called tip-substrate cyclic voltammetry (T/S CV), has been used to investigate the film shows negative feedback behavior, since the  $\text{Os}(\text{bpy})_3^{2+}$  formed is unable to oxidize tip-generated  $\text{Fe}(\text{CN})_6^{4-}$  back to  $\text{Fe}(\text{CN})_6^{3-}$ .

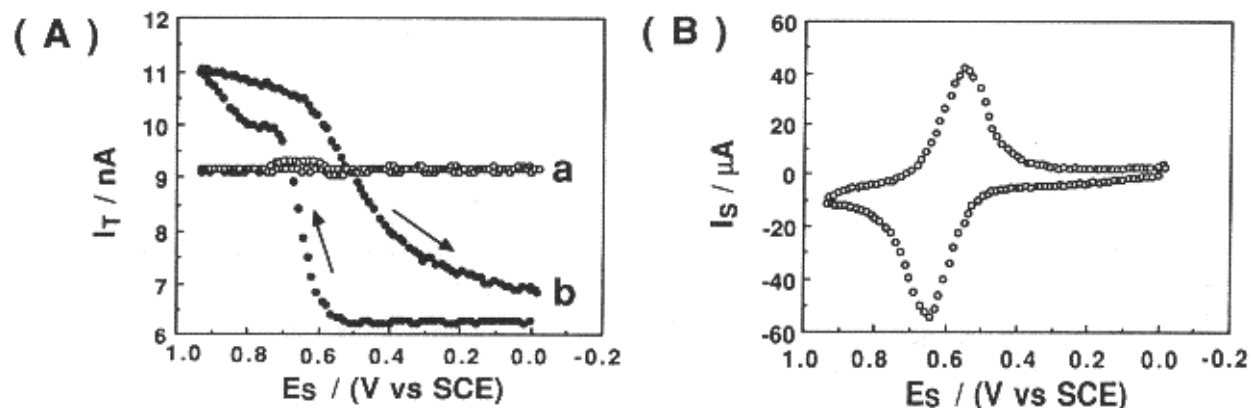


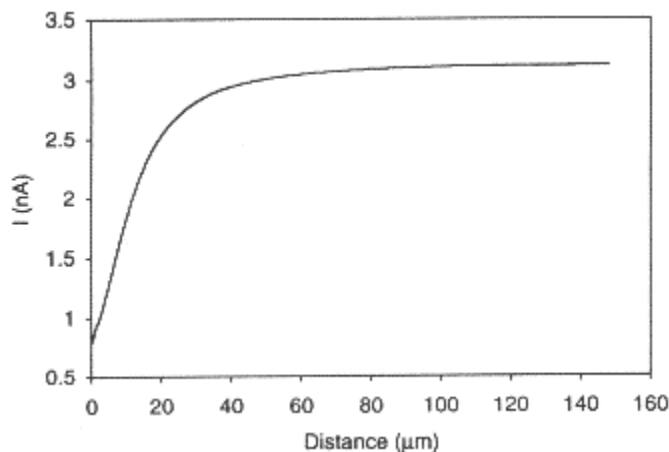
**Figure 6.** T/S CVs (A) curve a,  $d = 500 \mu\text{m}$ , and substrate CV (B) on Nafion/Os(bpy) $_3^{3+/2+}$  electrode in  $\text{K}_3\text{Fe}(\text{CN})_6/\text{Na}_2\text{SO}_4$ , scan rate = 50 mV/sec,  $E_T = -0.4 \text{ V}$  vs. SCE. (Reprinted with permission from Ref. 6a, copyright 1990, American Chemical Society.)

electrochemical behavior of an Os(bpy) $_3^{2+}$ -incorporated Nafion film.<sup>6a</sup> T/S CV involves monitoring the tip current vs. the substrate potential ( $E_S$ ) while the tip potential ( $E_T$ ) is maintained at a given value and the tip is held near the substrate. The substrate CV ( $i_s$  vs.  $E_S$ ) of an Os(bpy) $_3^{2+}$ -incorporated Nafion film covering a Pt disk electrode in  $\text{Fe}(\text{CN})_6^{3-}$  solution only shows a wave for the Os(bpy) $_3^{2+/3+}$  couple (Fig. 6B), indicating the permselectivity of the Nafion coating. Fig. 6A shows the corresponding T/S CV curves. When the tip is far from the substrate,  $i_T$  is essentially independent of  $E_S$ . When the tip is close to the substrate ( $d = 10 \mu\text{m}$ ), either negative or positive feedback effects are observed, depending on the oxidation state of the Os(bpy) $_3^{2+/3+}$  couple in the Nafion. When  $E_S$  is swept positive of the Os(bpy) $_3^{2+/3+}$  redox wave, a positive feedback effect is observed due to the regeneration of  $\text{Fe}(\text{CN})_6^{3-}$  in the solution gap region because of the oxidation of  $\text{Fe}(\text{CN})_6^{4-}$  by Os(bpy) $_3^{3+}$  at the solution-film interface. When  $E_S$  is negative of the redox wave,

### E. Liquid-liquid interfaces

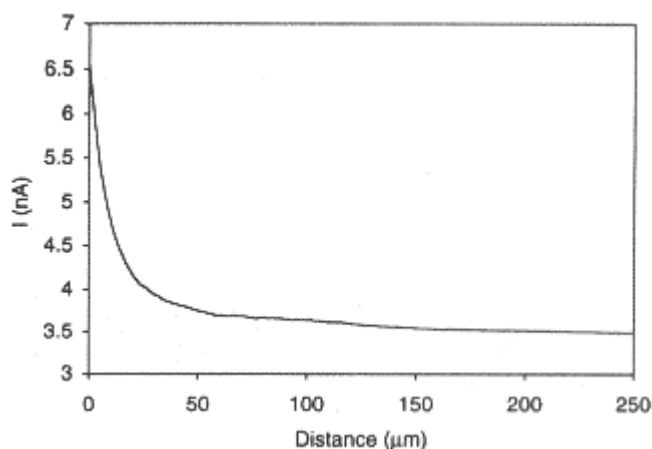
One of the most promising applications of SECM is the study of charge transport at the interface between two immiscible electrolyte solution (ITIES).<sup>7</sup> Unlike conventional techniques, SECM allows for the studies of both ion and electron transfer at the interface. For example, uphill electron transfer, in which an electron is transferred uphill from a redox couple with a higher standard reduction potential in one phase to another redox couple having a lower standard reduction potential in a second immiscible phase has been demonstrated using the system TCNQ (in 1,2-dichloroethane (DCE))/ferrocyanide (in water).<sup>7c</sup> Fig. 7 shows the approach curve obtained as the UME approaches the interface when the system contains supporting electrolytes with no partitioning ions such as tetraphenylarsonium (TPAs $^+$ ). However, the reverse electron flow for the same redox reaction can be induced by employing TPAs $^+$  as a potential-determining ion as shown in Fig. 8. The driving force for this reverse electron transfer is the imposition of an interfacial potential difference by the presence in solution of TPAs $^+$  in both phases ( $\Delta_o^w\phi = -364 \text{ mV}$ ). Note that the detection of reverse electron flow in this case could not be done using the method commonly used for studies of the ITIES, e.g., cyclic voltammetry.

**Figure 7.** Approach mM TCNQ and 1 mM  $\text{Fe}(\text{CN})_6^{3-}$  and 0.1 the absence of electron liquid/liquid interface. microelectrode was used the electrode tip from potential,  $-0.4 \text{ V}$  vs with permission from American Chemical



curve for the system: 10 TPAsTPB in DCE // 1 M LiCl in  $\text{H}_2\text{O}$ , showing transfer across the A 25- $\mu\text{m}$ -diameter Pt to generate  $\text{Fe}(\text{CN})_6^{4-}$  at the  $\text{Fe}(\text{CN})_6^{3-}$ . Tip Ag/AgCl. (Reprinted Ref. 7c, copyright 1995, Society.)

**Figure 8.** Approach curve for TCNQ and 1 mM TPAsTPB in  $\text{Fe}(\text{CN})_6^{3-}$ , 0.1 M LiCl and 1  $\text{H}_2\text{O}$ , showing reverse electron phase transfer catalyst  $\text{TPAs}^+$ . V vs Ag/AgCl. (Reprinted with Ref. 7c, copyright 1995, Chemical Society.)



the system: 10 mM DCE // 1 mM mM TPAsCl in transfer driven by Tip potential, -0.4 permission from American

Since the ITIES is not polarizable in the presence of  $\text{TPAs}^+$  in both phases, any attempt to impose externally a potential across the interface with electrodes in two phases would result in interfacial ion transfer and a current flow. The SECM approach does not suffer from this interference. Charge transfer processes across the ITIES with or without membranes have also been studied.

#### F. Probing patterned biological systems

SECM has been actively employed to probe artificially or naturally patterned biological systems.<sup>8</sup> Both amperometric and potentiometric techniques with ion-selective tips can be used. A direct test of the SECM's ability to image an enzymatic reaction over a localized surface region<sup>8a</sup> is shown in Fig. 9. Glucose oxidase (GO) hydrogel was filled inside small, well-defined pores of polycarbonate filtration membranes. The buffered assay solution contained a high concentration of D-glucose as well as two redox mediators, methyl viologen dication ( $\text{MV}^{2+}$ ) and neutral hydroquinone ( $\text{H}_2\text{Q}$ ). Fig. 9a shows an image obtained with a tip potential of -0.95 V vs. a silver quasi reference electrode (AgQRE) where  $\text{MV}^{2+}$  was reduced to  $\text{MV}^+$ . Since  $\text{MV}^+$  does not react with reduced GO at the hydrogel-filled region, a negative feedback current was obtained. However, with the tip potential changed to 0.82 V, where hydroquinone was oxidized to p-benzoquinone by reduced GO, an increased tip current was observed (Fig. 9b). This positive feedback current over the hydrogel region indicates a significant catalytic feedback of the hydroquinone and provides a direct image of the local enzymatic reaction.

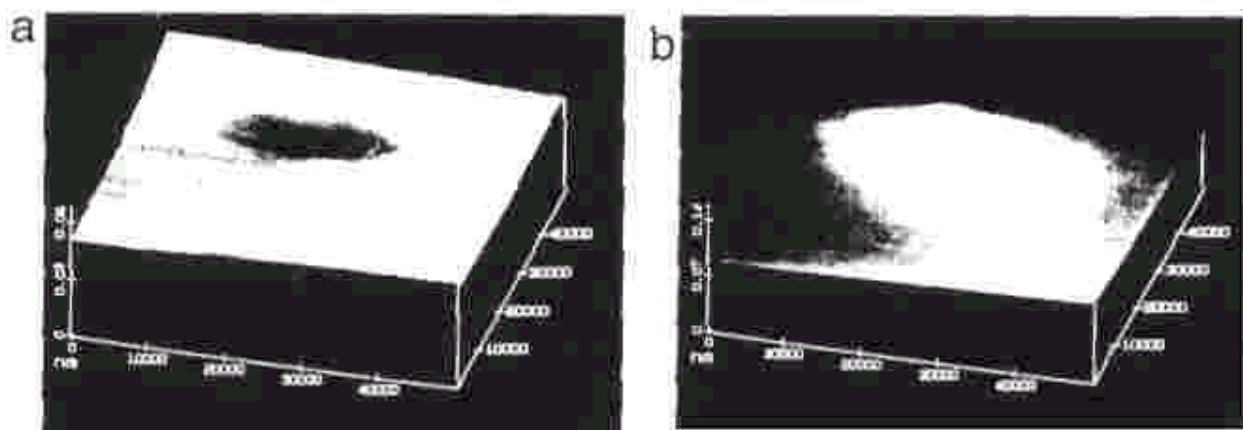


**Figure 9.** SECM images ( $50 \mu\text{m} \times 50 \mu\text{m}$ ) of a single GO hydrogel-filled pore on the surface of a treated membrane. Images were taken with a carbon microelectrode tip ( $a = 4.0 \mu\text{m}$ ). (a). Negative feedback with  $\text{MV}^{2+}$  mediator at tip potential -0.95 V vs AgQRE. (b). Positive feedback with hydroquinone mediator at tip potential +0.82 V vs AgQRE in 0.1 M phosphate-perchlorate buffer (pH 7.0) containing 100 mM D-glucose, 50  $\mu\text{M}$  hydroquinone and 0.1 mM  $\text{MVCl}_2$ . Lightest image regions depict the greatest tip current. (Reprinted with permission from Ref. 8a, copyright 1993, American Chemical Society.)

### G. Fabrication

The SECM can be used to fabricate microstructures on surfaces by deposition of metal or other solids or by etching of the substrate.<sup>9</sup> Two different approaches have been used, the direct mode<sup>9a,b</sup> and the feedback mode<sup>9c</sup>. Typically, in the direct mode, the tip, held in close proximity to the substrate, acts as a working electrode (in deposition reactions) or as the counterelectrode (in etching processes). The feedback mode of fabrication utilizes the same arrangement as in SECM imaging.

The tip reaction is selected to generate a species that reacts at the substrate to promote the desired reaction, i.e., deposition or etching. For example, a strong oxidant, like Br<sub>2</sub>, generated at the tip can etch the area of the substrate, e.g., GaAs, directly beneath the tip.<sup>9d</sup> The mediator reactant is chosen to be one that reacts completely and rapidly at the substrate, thus confining the reaction to a small area on the substrate and producing features of area near that of the tip. Small tip size and close tip-substrate spacing are required for high resolution.

### III. References

1. (a). A. J. Bard, F.-R. F. Fan, J. Kwak, and O. Lev, *Anal. Chem.* **1989**, *61*, 132; (b). A. J. Bard, F.-R. F. Fan, and M. V. Mirkin in *Electroanalytical Chemistry*, Vol.18 (A. J. Bard, ed.), Marcel Dekker, New York, 1994, p. 243.
2. e.g., (a). For a review of early potentiometric SECM experiments, see Ref. 1b; (b). C. Wei, A. J. Bard, G. Nagy, and K. Toth, *Anal. Chem.* **1995**, *67*, 1346; (c). K. Toth, G. Nagy, C. Wei, and A. J. Bard, *Electroanal.* **1995**, *7*, 801; (d). M. Kupper and J. W. Schultze, *Fres. J. Anal. Chem.* **1996**, *356*, 187.
3. See also (a). R. C. Engstrom, M. Weber, D. J. Wunder, R. Burgess, and S. Winquist, *Anal. Chem.* **1986**, *58*, 844; (b). R. C. Engstrom, T. Meaney, R. Tople, and R. M. Wightman, *Anal. Chem.* **1987**, *59*, 2005.
4. e.g., (a). D. O. Wipf and A. J. Bard, *J. Electrochem. Soc.* **1991**, *138*, 469; (b). B. R. Horrocks, M. V. Mirkin, and A. J. Bard, *J. Phys. Chem.* **1994**, *98*, 9106; (c). R. S. Hutton and D. E. Williams, *Electrochim. Acta*, **1994**, *39*, 701; (d). N. Casillas, P. James, and W. H. Smyrl, *J. Electrochem. Soc.* **1995**, *142*, L16; (e). M. V. Mirkin, T. C. Richards, and A. J. Bard, *J. Phys. Chem.* **1993**, *97*, 7672; (f). M. V. Mirkin, L.O.S. Bulhoes, and A. J. Bard, *J. Am. Chem. Soc.* **1993**, *115*, 201; (g). J. V. Macpherson, M. A. Beeston, and P. R. Unwin, *J. Chem. Soc. Faraday Trans.* **1995**, *91*, 899.
5. e.g., (a). F. M. Zhou, P. R. Unwin, and A. J. Bard, *J. Phys. Chem.* **1992**, *96*, 4917; (b). P.R. Unwin and A. J. Bard, *J. Phys. Chem.* **1991**, *95*, 7814; (c). F. M. Zhou and A. J. Bard, *J. Am Chem. Soc.* **1994**, *116*, 393; (d). D. A. Treichel, M. V. Mirkin, and A. J. Bard, *J. Phys. Chem.* **1994**, *98*, 5751; (e). C. *100*, 17881; (f). C. J. Slevin, J. A. Umbers, J. H. Demaille, P. R. Unwin, and A. J. Bard, *J. Phys. Chem.* **1996**, *100*, 14137.
6. e.g., (a). C. Lee and A. J. Bard, *Anal. Chem.* **1990**, *62*, 1906; (b). C. Lee, J. Kwak, and F. C. Anson, *Anal. Chem.* **1991**, *63*, 1501; (c). J. Kwak, C. Lee, and A. J. Bard, *J. Electrochem. Soc.* **1990**, *137*, 1481; (d). C. Lee and F. C. Anson, *Anal. Chem.* **1992**, *64*, 250. (e). I. C. Jeon and F. C. Anson, *Anal. Chem.* **1992**, *64*, 2021; (f). M. V. Mirkin, F.-R. F. Fan, and A. J. Bard, *Science*, **1992**, *257*, 364. (g). M. Arca, M. V. Mirkin, and A. J. Bard, *J. Phys. Chem.* **1995**, *99*, 5040; (h). M. Pyo and A. J. Bard, *Electrochim. Acta* **1997**, *42*, 3077; (i). E. R. Scott, A. I. Laplaza, H. S. White, and J. B. Phipps, *Pharmaceut. Res.* **1993**, *10*, 1699; (j). S. R. Snyder and H. S. White, *J. Electroanal. Chem.* **1995**, *394*, 177; (k). S. B. Basame and H. S. White, *J. Phys. Chem.* **1995**, *99*, 16430; (l). N. Casillas, S. Charlebois, W. H. Smyrl, and H. S. White, *J. Electrochem. Soc.* **1994**, *141*, 636; (m). D. O. Wipf, *Colloid Surf. A*, **1994**, *93*, 251. (n). E. R. Scott, H. S. White, and J. B. Phipps, *Solid State Ionics* **1992**, *53*, 176; (o). S. Nugnes and G. Denuault, *J. Electroanal. Chem.* **1996**, *408*, 125; (p). M. H. T. Frank and G. Denuault, *J. Electroanal. Chem.* **1993**, *354*, 331; (q). J. V. Macpherson and P. R. Unwin, *J. Chem. Soc. Faraday Trans.* **1993**, *89*, 1883; (r). J. V. Macpherson and P. R. Unwin, *J. Phys. Chem.* **1994**, *98*, 1704; (s). J. V. Macpherson and P. R. Unwin, *J. Phys. Chem.* **1995**, *99*, 14824; **1996**, *100*, 19475; (t). J. V. Macpherson, C. J. Slevin, and P. R. Unwin, *J. Chem. Soc. Faraday Trans.* **1996**, *92*, 3799; (u). K. Borgwarth, C. Ricken, D. G. Ebling, and Heinze, *Ber. Bunsenges. Phys. Chem.* **1995**, *99*, 1421; (v). Y. Y. Zhu and D. E. Williams, *J. Electrochem. Soc.* **1997**, *144*, L43; (w). C. Jehoulet, Y. S. Obeng, Y. T. Kim, F. M. Zhou, and A. J. Bard, *J. Am. Chem. Soc.* **1992**, *114*, 4237; (x). E. R. Scott, H. S. White, and J. B. Phipps, *J. Membrane Sci.* **1991**, *58*, 71; (y). H. Sugimura, T. Uchida, N. Kitamura, and H. Masuhara, *J. Phys. Chem.* **1994**, *98*, 4352; (z). J. E. Vitt and R. C. Engstrom, *Anal. Chem.* **1997**, *69*, 1070.
7. e.g., (a). C. Wei, A. J. Bard, and M. V. Mirkin, *J. Phys. Chem.* **1995**, *99*, 16033; (b). T. Solomon and A. J. Bard, *J. Phys. Chem.* **1995**, *67*, 2787; (c). T. Solomon and A. J. Bard, *J. Phys. Chem.* **1995**, *99*, 17487; (d). Y. Selzer and D. Mandler, *J. Electroanal. Chem.* **1996**, *409*, 15; (e). M. Tsionsky, A. J. Bard, and M. V. Mirkin, *J. Phys. Chem.* **1996**, Atherton, and P. R. Unwin, *J. Chem. Soc. Faraday Trans.* **1996**, *92*, 5177; (g). Y. H. Shao, M. V. Mirkin, and J. F. Rusling, *J. Phys. Chem. B* **1997**, *101*, 3202; (h). M. Tsionsky, A. J. Bard, and M. V. Mirkin, *J. Am. Chem. Soc.* **1997**, *119*, 10785; (i). M.-H. Delville, M. Tsionsky, and A. J. Bard, (submitted to *J. Am. Chem. Soc.* for publication).

8. e.g., (a). D. T. Pierce and A. J. Bard, *Anal. Chem.* **1993**, *65*, 3598; (b). B. R. Horrocks, D. Schmidtke, A. Heller, and A. J. Bard, *Anal. Chem.* **1993**, *65*, 3605; (c). H. Yamada, H. Shiku, T. Matsue, and I. Uchida, *Bioelectrochem. Bioenerg.* **1994**, *33*, 91; (d). B. Grundig, G. Wittstock, U. Rudel, and B. Strehlitz, *J. Electroanal. Chem.* **1995**, *395*, 143; (e). G. Wittstock, K. J. Yu, H. B. Halsall, T. H. Ridgway, and W. R. Heineman, *Anal. Chem.* **1995**, *67*, 3578; (f). H. Shiku, T. Matsue, and I. Uchida, *Anal. Chem.* **1996**, *68*, 1276; (g). J. L. Gilbert, S. M. Smith, and E. P. Lautenschlager, *J. Biomed. Mater. Res.* **1993**, *27*, 1357; (h). C. Kranz, T. Lotzbeyer, H. L. Schmidt, and W. Schuhmann, *Biosens. Bioelectron.* **1997**, *12*, 257; (i). C. Kranz, G. Wittstock, H. Wohlschlager, and W. Schuhmann, *Electrochim. Acta*, **1997**, *42*, 3105; (j). C. Lee, J. Kwak, and A. J. Bard, *Proc. Natl. Acad. Sci. U.S.A.* **1990**, *87*, 1740; (k). R. B. Jackson, M. Tsionsky, Z. G. Cardon, and A. J. Bard, *Plant Physiol.* **1996**, *112*, 354; (l). M. Tsionsky, Z. G. Cardon, A. J. Bard, and R. B. Jackson, *Plant Physiol.* **1997**, *113*, 895.
9. e.g., (a). C. W. Lin, F.-R. F. Fan, and A. J. Bard, *J. Electrochem. Soc.* **1987**, *134*, 1038; (b). D. H. Craston, C. W. Lin, and A. J. Bard, *J. Electrochem. Soc.* **1988**, *135*, 785; (c). D. Mandler and A. J. Bard, *J. Electrochem. Soc.* **1989**, *136*, 3143; (d). D. Mandler and A. J. Bard, *J. Electrochem. Soc.* **1990**, *137*, 2468; (e). O. E. Husser, D. H. Craston, and A. J. Bard, *J. Vac. Sci. Technol. B* **1988**, *6*, 1873; (f). Y.-M. Wu, F.-R. F. Fan, and A. J. Bard, *J. Electrochem. Soc.* **1989**, *136*, 885; (g). H. Sugimura, T. Uchida, N. Shimo, N. Kitamura, and H. Masuhara, *Ultramicroscopy* **1992**, *42*, 468; (h). I. Shohat and D. Mandler, *J. Electrochem. Soc.* **1994**, *141*, 995; (i). S. Meltzer and D. Mandler, *J. Chem. Soc. Faraday Trans.* **1995**, *91*, 1019; (j). C. Kranz, H. E. Gaub, and W. Schuhmann, *Advan. Mater.* **1996**, *8*, 634; (k). J. F. Zhou and D. O. Wipf, *J. Electrochem. Soc.* **1997**, *144*, 1202.

## Other Electrochemical Instruments

CH Instruments provides a full line of electrochemical instrumentation besides the CHI900 SECM. Our Model 500 is dedicated to ac measurements. The Model 600A series are for general purpose electrochemical measurements. The Model 700 series bipotentiostat can be used for rotating ring-disk electrodes (RRDE) and other cases where dual channel measurements are essential. The Model 800 series are suitable for either single or dual channel flow cell detection and LCEC, and the bipotentiostat can also be used for an RRDE. We just upgraded our Model 600 series to Model 600A series. The new model has a higher sensitivity ( $1 \times 10^{-12}$  A/V). It also uses a four-electrode configuration, with the 4th electrode used as a sensing electrode to overcome the contact resistance. This is particularly important in high current measurements. An auxiliary measurement channel is added for simultaneous recording of other signals, such as spectroscopic signals. The performance of AC impedance is also improved.

All the instrument models are controlled by an external PC under the Windows environment. They have very similar software features as the CHI900 SECM described in this brochure.

The following two tables describe the functions, specifications and experiment dynamic ranges of various series.

### Functions of Various Instrument Models

Functions	600A Series	700 Series	800 Series	800A Series
Cyclic Voltammetry	●	●	●	●
Linear Sweep Voltammetry <sup>&amp;</sup>	●	●	●	●
Staircase Voltammetry <sup>#, &amp;</sup>	●	●		
Tafel Plot	●	●		
Chronoamperometry	●	●	●	●
Chronocoulometry	●	●	●	●
Differential Pulse Voltammetry <sup>#, &amp;</sup>	●	●	●	●
Normal Pulse Voltammetry <sup>#, &amp;</sup>	●	●	●	●
Differential Normal Pulse Voltammetry <sup>#, &amp;</sup>	●			
Square Wave Voltammetry <sup>&amp;</sup>	●	●	●	●
AC Voltammetry <sup>#, &amp;, \$</sup>	●	●		
2nd Harmonic AC Voltammetry <sup>#, &amp;, \$</sup>	●	●		
Amperometric I-t Curve	●	●	●	●
Differential Pulse Amperometry	●		●	●
Double Differential Pulse Amperometry	●		●	●
Triple Pulse Amperometry	●		●	●

Bulk Electrolysis with Coulometry	●	●	●	●
Hydrodynamic Modulation Voltammetry	●	●		
AC Impedance	●	●		
Impedance - Time	●	●		
Chronopotentiometry	●			
Chronopotentiometry with Current Ramp	●			
Potentiometric Stripping Analysis	●		●	●
Galvanostat	●			
Bipotentiostat		●	●	●
iR Compensation	●			
RDE control (0-10V output)	●	●		
External Potential Input	●			
Auxiliary Signal Measurement Channel	●			
CV simulator	●	●	●	●

#: Corresponding polarographic mode can be performed. &: Corresponding stripping mode can be performed.

\$. Phase selective data are available.

\*: The above list are for the top model of each series. For each instrument series, we provide various models to suit different needs and budgets. For more details of different models, please contact us.

### ***Hardware Specifications and Dynamic Range of Experimental Parameters of Various Instrument Models***

Parameters	600A Series	700 Series	800 Series	800A Series
Potentiostat rise time	< 2 $\mu$ s	< 2 $\mu$ s		
Potential Range (V)	$\pm 10$	$\pm 10$	$\pm 2$	$\pm 3.275$
Compliance voltage (V)	$\pm 12$	$\pm 12$	$\pm 12$	$\pm 12$
Current (A)	$\pm 0.25$	$\pm 0.25$	$\pm 0.01$	$\pm 0.01$
Input impedance of reference electrode	$10^{12} \Omega$	$10^{12} \Omega$	$10^{12} \Omega$	$10^{12} \Omega$
Minimum potential increment	100 $\mu$ V	100 $\mu$ V	1 mV	100 $\mu$ V
Maximum potential update rate	5 MHz	4 MHz	500 Hz	500 Hz
ADC Resolution @ 1K Hz	20-bit		12-bit	20-bit
ADC Resolution @ 10 Hz	24-bit		24-bit	24-bit
Maximum sampling rate (Hz)	500K	333K	500	1000
Highest Sensitivity (A/V)	$1 \times 10^{-12}$	$1 \times 10^{-7}$	$5 \times 10^{-11}$	$1 \times 10^{-12}$
Scan rate (V/s) in CV	0.000001 to 5000	0.000001 to 2000	0.000001 to 0.5	0.000001 to 0.5
Pulse width (sec) in CA, CC	0.0001 to 1000	0.0002 to 1000	0.1 to 1000	0.1 to 1000
Pulse width (sec) in DPV, NPV	0.001 to 10	0.001 to 10	0.02 to 10	0.02 to 10
Frequency (Hz) in SWV	1 to 100000	1 to 100000	1 to 40	1 to 40
Frequency (Hz) in ACV	1 to 10000	1 to 10000		
Frequency (Hz) in SHACV	1 to 1000	1 to 1000		
Frequency (Hz) in IMP	0.0001 to 100K	0.0001 to 100K		

## Other Related Products

**Model 200 Picoamp Booster & Faraday Cage:** Allow current measurements down to 1 pA. Fully automatic and compatible with the Model 600A series and Model 700 series (single channel only) instruments.

**Model 680 Amp Booster:** Allows  $\pm 2$ A current and  $\pm 26$  volt compliance voltage. Fully automatic and compatible with the Model 600A series instruments.

### **Warranty:**

One-year warranty on electronic parts and labor, 90-day warranty on mechanical parts.

### **Demo Disk:**

Free Demo Disk available upon request. Please call, fax or e-mail us and state the model you are interested in and your applications.






Sept. 12, 1997 17:46:35  
 Tech: SECM  
 File: 912-2sec.bin  
 Probe E (V) = 0.4  
 Sensitivity (A/V) = 1e-9  
 X Distance (μm) = 100  
 Y Distance (μm) = 100  
 Incr. Dist. (μm) = 1  
 Incr. Time (s) = 0.0333  
 Long Move = X  
 End i Ratio (%) = 40  
 Max Incr (μm) = 0.5  
 Withdraw Dist (μm) = 50  
 Quiet Time (s) = 2

To further discuss with us our instruments and application possibilities, please contact us using the details below

In Europe please contact:

I J Cambria Scientific ♦ 11 Gwscwm Road ♦ Burry Port ♦ Carmarthen ♦ SA16 OBS . UK  
 Phone: 01554 835050 ♦ Fax: 01554 835060 ♦ E-mail: [info@ijcambria.com](mailto:info@ijcambria.com)  
 (Mobile: 07957 287343)  
 IJ Cambria Scientific: [www.ijcambria.com](http://www.ijcambria.com)

In the US please contact:

 CH Instruments, Inc.  
 3700 Tennyson Hill Drive · Austin, TX 78738 · USA  
 Tel: (512) 402-0176 · Fax: (512) 402-0186  
 E-mail: [info@chinstruments.com](mailto:info@chinstruments.com)